ISSN 2179-3956

EVALUATION OF TRIBOELECTRICITY IN DIAMOND-LIKE COATINGS CONTAINING SILVER NANOPARTICLES USING AFM AND KPFM*

Lucia Vieira[1]
Homero Santiago Maciel[1]
Rodrigo Savio Pessoa[1]
Thaisa Baesso Santos[2]

Abstract
Kelvin probe force microscopy (KPFM) can be used to monitor electrostatic charges on the surfaces of materials. In this paper, we describe the use of KPFM to evaluate the electrostatic effect induced by silver nanoparticles incorporated as clusters in diamond-like carbon (DLC) films, before and after scratching. The results are compared to those obtained for DLC films without silver nanoparticles. Raman spectroscopy was used to identify the DLC signature, and energy dispersive X-ray spectroscopy (EDX) was used to confirm the presence of silver in the film. The morphology of the DLC film containing silver was investigated using scanning electron microscopy (SEM) and transmission electron microscopy (TEM). The findings suggest that the incorporation of silver nanoparticles in amorphous materials could offer new options for electrostatic energy storage on the surfaces of these materials.
Keywords: Triboelectricity; Diamond-like carbon; Kelvin probe force microscopy; Nanoscale scratching.

[1] *Lecturer, Materials Science Department, UNIVAP, Fundamental Science Department, ITA, São José dos Campos, SP, Brazil.*
[2] *Master's degree student, Materials Science Department, UNIVAP, São José dos Campos, SP, Brazil*

* *Technical contribution to the 2nd International Brazilian Conference on Tribology – TriboBR 2014, November 3rd to 5th, 2014, Foz do Iguaçu, PR, Brazil.*

ISSN 2179-3956

1 INTRODUCTION

The triboelectric effect, also known as triboelectric charging, is a type of contact electrification whereby certain materials become electrically charged due to friction after coming into contact with another different material. Rubbing glass with fur, or passing a comb through the hair, can build up triboelectricity. The first triboelectric series was published by John Carl Wilcke in a 1757 paper on static charges, and the series list was later improved by other researchers [1]. Irwin Singer observed that the sliding friction process increases energy dissipation at the atomic scale [2]. This was also demonstrated by Baytekin et al., who found that electrified surfaces have charge distributions with either positive or negative polarity, comprising a random mosaic of oppositely charged regions with nanoscopic dimensions [3].

The mechanisms of electrical charge storage and dissipation have received considerable attention, because electrical charging is important in areas such as printing, electrostatic painting, and biological corrosion, and because static electricity can harm electronic devices, including instruments on satellites [4-7]. Damage to instrumentation, fires, and explosions can occur due to a lack of understanding of electrostatic phenomena.

Methods for detection of charging in insulators have been proposed based on microscopy techniques such as Kelvin probe force microscopy (KPFM) and atomic force microscopy (AFM) [6]. KPFM provides a useful means of monitoring electrical behavior in an insulator film and detecting charge carriers [4,5]. Recent studies using KPFM have shown that insulators contain electrical domains with excess fixed ions forming different potential distribution patterns, which can be imaged by potential mapping. Contrary to common assumptions, it has been shown that solid insulators are rarely electroneutral [7].

This paper concerns the detection and mapping of charging in diamond-like carbon films doped with silver (DLC-Ag). We describe triboelectric effects associated with scratch testing conducted at the nanoscale. Normal loads were applied using a cube-corner diamond tip with a radius of curvature smaller than 50 µm, allied with atomic force microscopy. This enabled observation of structural defects [8], together with analyses of applied force, scratch speed, temperature, friction coefficient, and scratch morphology [9-12].

2 Materials and Methods

DLC-Ag coatings with a thickness of 1.5 µm were deposited by plasma-enhanced chemical vapor deposition (PECVD), using a Model NPE-4000 system (Nano-Master Inc., Austin, TX, USA). The plasma discharge utilized a load-lock parallel plate reactor with a Pinnacle Plus power supply (Advanced Energy), and the operating parameters were controlled by computer. The film was deposited onto a silicon substrate (n-Si (100); $\rho < 0.004$ Ω cm), as described elsewhere [13].

The nanoscale scratch testing employed a DLC-Ag film deposited on the silicon substrate. The scratch was performed using a MultiMode III AFM (Bruker) with a diamond tip (Model DNISP-MM). In order to ensure good repeatability in scratch testing at the nanoscale, it is necessary to control the normal load and the tip sensitivity. In the present case, a constant normal load of 30 µN was employed. This normal force (F) was calculated indirectly using Equation 1, as described previously [14,15].

---

* *Technical contribution to the 2nd International Brazilian Conference on Tribology – TriboBR 2014, November 3rd to 5th, 2014, Foz do Iguaçu, PR, Brazil.*

ISSN 2179-3956

$$F = k\frac{(Stp - Stp\,\emptyset)}{SAB} \qquad \text{(Equation 1)}$$

In Equation 1, *k* is the cantilever spring constant, calculated by the Sader method [16]; *Stp* is the set point value (in volts), calculated from a predetermined normal force; *Stpø* is the set point zero (in volts), calculated from the force plot, corresponding to the voltage with the tip touching the sample surface without any applied normal force; and *SAB* is the sensitivity (in volts/nm), calculated from the force plot as recommended in the AFM instrument manual.
The tip velocity was 0.1 µm/s, and the normal force applied with the diamond tip was 30 µN. Figure 1 shows two images, where Figure 1(a) is a view of the contact interaction between the tip and the surface, with an adhesion component. Figure 1(b) shows a tip force calibration plot for a hard surface without any adhesion between the sample and tip. This image was used to measure the voltage shifts in the X and Y directions. The error probability for the X-axis, using relative frequency, was determined by Equation 2.

$$p = \Delta S/A \qquad \text{(Equation 2)}$$

Where ΔS is the distance between two pixels, and A is the area, for AFM images constructed based on the force calibration plot. In Figure 1(b), the Y-axis represents the deflection of the tip under 0.15 V/nm, and the X-axis shows divisions of 15 nm distributed over 45 µm^2. It can be seen that there was no component corresponding to adhesion between the tip and the surface.
All the AFM experiments were conducted with the humidity of the environment controlled to below 20%, using a dry nitrogen atmosphere. This enabled a calibration curve to be obtained without the interference of a layer of water between the tip and the sample surface, as shown in Figure 1(b).

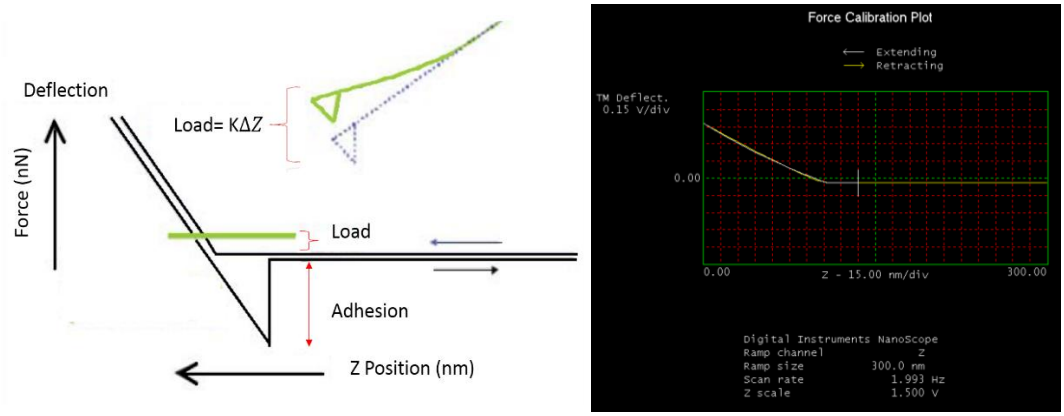

(a) (b)

Figure 1. (a) Schematic view of the AFM experimental setup, and (b) typical force calibration plot for a hard surface, with no adhesion between the tip and the surface.

In order to ensure the reproducibility of the normal force in all measurements, it was necessary to repeat the tip sensitivity procedure for each new setup. The tip sensitivity changed according to the position of the laser spot on the diamond tip. Figure 2 shows an SEM image of a portion of the cantilever including the diamond tip used to produce the scratch track by means of surface contact with controlled normal force. The shape of the tip resulted in nanoscale track morphology. The present work

* *Technical contribution to the 2nd International Brazilian Conference on Tribology – TriboBR 2014, November 3rd to 5th, 2014, Foz do Iguaçu, PR, Brazil.*

ISSN 2179-3956

employed a pyramidal diamond tip with a height of 50 μm, a front angle of 55 ± 2º, a back angle of 35 ± 2º, and a side angle of 51 ± 2º, as shown in Figure 2.

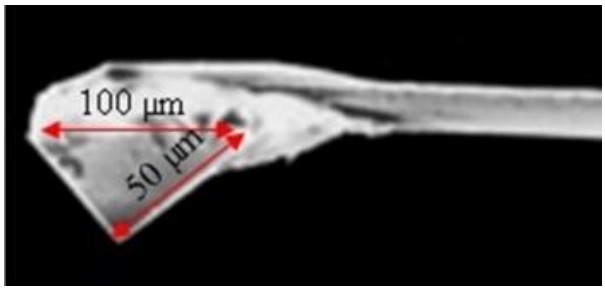

Figure 2. Scanning electron microscopy image showing part of the AFM cantilever and the configuration of the diamond tip.

After the nanoscale scratching, the AFM configuration was changed to the KPFM configuration, and a tip covered with a platinum coating replaced the diamond tip. The KPFM images were also obtained using the MultiMode AFM (Bruker). The surface topography and electric potential images were obtained simultaneously. During the sample slide, the mechanical oscillation of the probe was monitored by four photodetector quadrants and was analyzed using two feedback loops. The first loop controlled the distance between the tip and the sample while the tip scanned the surface at constant oscillation amplitude. The tip voltage was maintained at zero by adjusting the DC voltage feedback control. The second loop was used for the surface potential measurements, in non-contact mode. The electric field between the platinum tip and the sample was monitored and converted to electric potential images using grey-scale or color-coding.

The scratch area was located by marking it with a pen near the track. The images of the scratch morphology were recorded and the potential was analyzed according to the area and surface selected.

The atomic arrangement of the DLC-Ag film was first analyzed by Raman scattering spectroscopy, using a Renishaw 2000 system with an Ar^+ ion laser (λ = 514 nm), operated with backscattering geometry. The laser power on the sample was ~0.6 mW, and the diameter of the laser spot was 2.5 μm. The Raman shift was calibrated in relation to the diamond peak at 1332 cm^{-1}. All measurements were carried out in air at room temperature (21 ºC).

After the sclerometry process (scratching), the groove morphology was evaluated considering wear modes reported in the literature. The commonest types of wear for polymeric surfaces are abrasion, adherence, and fatigue [17]. However, given the interrelation between the different wear mechanisms during tip sliding, determination of the wear mechanism is not straightforward and a rigorous wear evaluation needs to consider a narrow range of contact variables, such as tip geometry, applied load, velocity, and temperature at the sliding contact [18].

As a simplistic definition, abrasion occurs when a harder material acts on the polymer film causing scratches or gouging. This can be due to abrasive particles cutting the film due to plastic grooving in which case all the material displaced is removed in the form of a chip, as shown in Figure 3(a), or ploughing, in which material is pushed ahead of the particle and displaced sideways to form ridges adjacent to the groove. The morphological effect of “ploughing” is shown in Figure 3(b). Finally, the “plastic grooving” effect is shown in Figure 3(c), where all the material is removed from the film [17,18]. These wear modes were used to evaluate the wear for the groove shown in Figure 5(b).

* *Technical contribution to the 2nd International Brazilian Conference on Tribology – TriboBR 2014, November 3rd to 5th, 2014, Foz do Iguaçu, PR, Brazil.*

ISSN 2179-3956

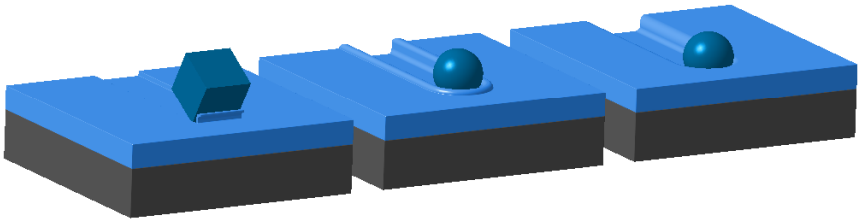

(a) (b) (c)

Figure 3. Schematic illustration of the wear modes used to evaluate the morphology of scratch grooves.

3 RESULTS AND DISCUSSION

3.1 Film analysis using Raman spectroscopy

The Raman shifts obtained for the DLC-Ag film (Figure 4) revealed the presence of carbon in ring-shaped clusters. According to the literature, DLC films present two characteristic bands, usually centered at 1350 cm^{-1} (D band) and 1580 cm^{-1} (G band) [19]. Here, the plots corresponding to the D and G bands displayed displacements towards the left, of 34 cm^{-1} (D band) and 40 cm^{-1} (G band). The Raman spectra for the DLC-Ag film presented the typical DLC signature, which confirmed that the cage used inside the reactor (as a source of Ag) did not change this signature. The only difference was the shift mentioned above, which was indicative of a coating rich in ring-shaped carbon.

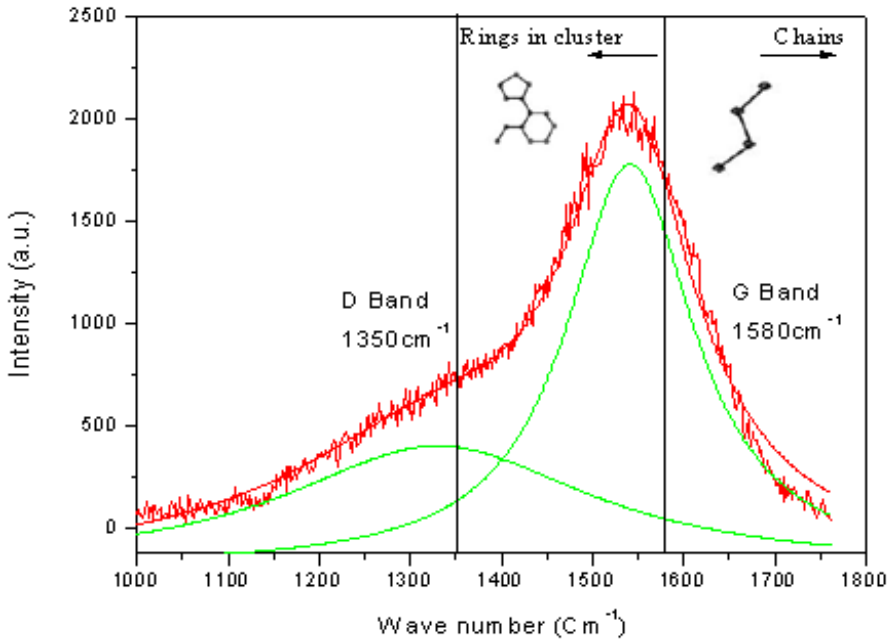

Figure 4. Raman spectrum of the DLC-Ag film. The original positions of the D and G bands are indicated by the black lines.

3.2 AFM Analysis of the DLC-Ag Film

Figure 5(a) shows an AFM image of the morphology of a 7 x 7 μm^2 area of the DLC-Ag film with a 5 µm length groove line produced using a diamond tip under 30 µN of normal force. The presence of silver in clusters can be observed as white dots in the

** Technical contribution to the 2nd International Brazilian Conference on Tribology – TriboBR 2014, November 3rd to 5th, 2014, Foz do Iguaçu, PR, Brazil.*

ISSN 2179-3956

image. Figure 5(b) shows a complementary KPFM near-surface voltage-mapping image of the same area, with values ranging from zero to 0.1 V. The dark regions indicate lower voltage values, while higher voltages are indicated in white-yellow (brighter colors). The colors appear brighter along the scratch and in its vicinity, reflecting higher potential values. This indicates that the scratch promoted electrical charge separation, enhancing the electric fields in the region. This phenomenon is typical of the triboelectric effect during sliding contact [5]. Also highlighted in this image is the local enhancement of the potential where the silver clusters were located. This revealed a remarkable capacity of the silver nanoparticles to promote electrostatic charging and enhancement of the surface electric field, consequently increasing the electrostatic energy that could be stored near the surface of the DLC-Ag films.

Figure 5(c) shows the three-dimensional scratch morphology. Figure 5(d) shows a build-up of material on the right-hand side of the groove, which is a common feature in ploughing wear caused by the accumulation of material derived from the scratch. From Figure 5(d), the width and depth of the V-type profile were 99.2 and 4.7 nm, respectively. Since the pyramidal diamond tip had a 100 µm base and a height of 50 µm, it could be concluded that penetration of the tip corresponded to less than 1% of its total height, confirming that a scratch on the 1.5 µm thick DLC-Ag coating formed a nano-groove.

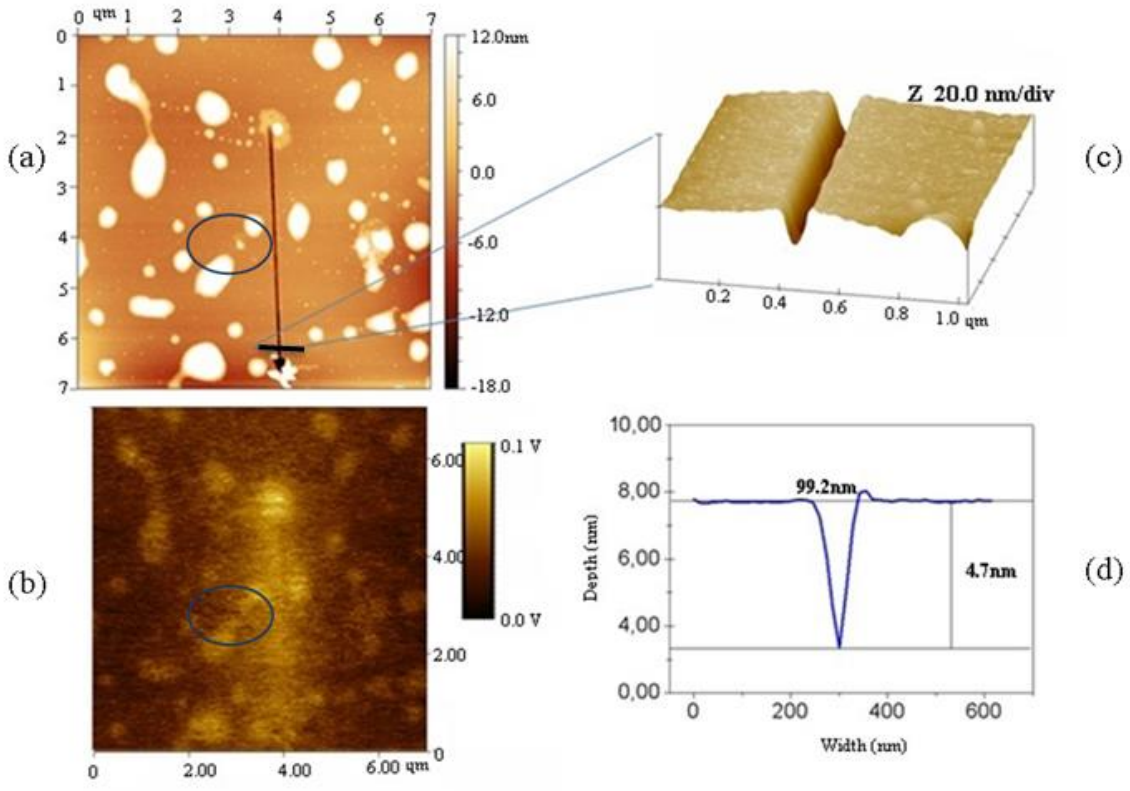

Figure 5. (a) AFM image of the DLC-Ag film in the vicinity of the scratch, showing connected silver clusters (e.g. in the blue circle); (b) KPFM voltage image of the same area, showing (in brighter colors) the scratch region and the connected silver clusters (blue circle); (c) scratch morphology in 3D; (d) scratch morphology profile with spatial dimensions.

A comparison of the electrostatic features of the DLC, DLC-Ag, and scratched DLC-Ag films is presented in Figure 6, which displays KPFM images of each film, together with the corresponding voltage profiles. The profiles were measured along the

ISSN 2179-3956

straight line shown in blue in the images of the 5 x 5 μm^2 areas. Figure 6(a) shows a voltage image of the DLC film. The lower contrast in this image indicates lower voltages, with an electric potential difference of around 0.030 V measured between the two points on the scan line indicated by the red arrows. Figure 6(b) shows a voltage image for the DLC-Ag film (with a potential difference of 0.050 V), where the silver clusters in the film can be seen as the brighter spots. These clusters acted to increase the variation of potential on the surface. Figure 6(c) shows a voltage image for the region of the groove (with an even greater potential difference of 0.068 V). A further five points were measured for each image (Table 1). The highest values were obtained for DLC-Ag. With scratching, the capacity of silver to act as a solid lubricant resulted in it spreading in the groove, hence enhancing the voltage values. The same effect was observed at the side of the cross-section with build-up of material, which was indicative of ploughing (as shown in Figure 5(d)).

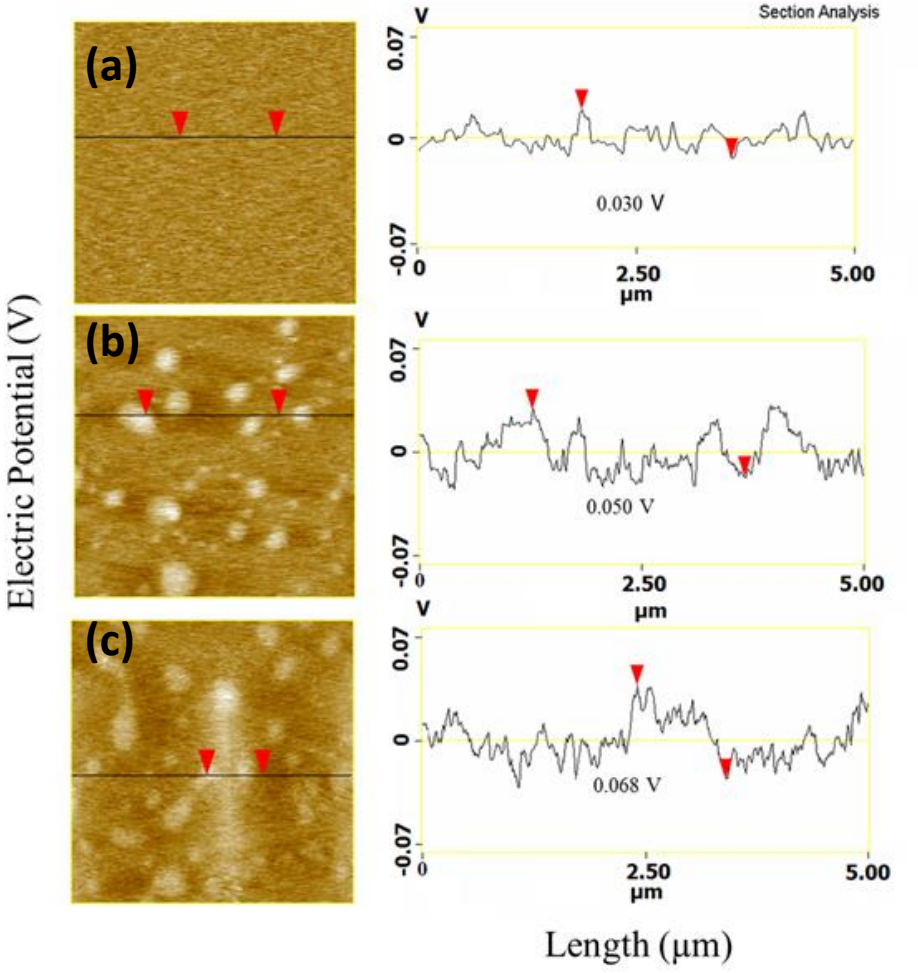

Figure 6. KPFM images with voltage contrast, and section analysis plots with potentials measured between the red arrows: (a) DLC film, (b) DLC-Ag film, (c) DLC-Ag film with scratch.

* *Technical contribution to the 2nd International Brazilian Conference on Tribology – TriboBR 2014, November 3rd to 5th, 2014, Foz do Iguaçu, PR, Brazil.*

ISSN 2179-3956

Table 1. Voltage measurements corresponding to the KPFM images of each sample: DLC film (yellow bars); DLC-Ag film (blue bars); and scratched DLC-Ag film (orange bars). Five measurements were made in each case. The associated errors bars were around 1%.

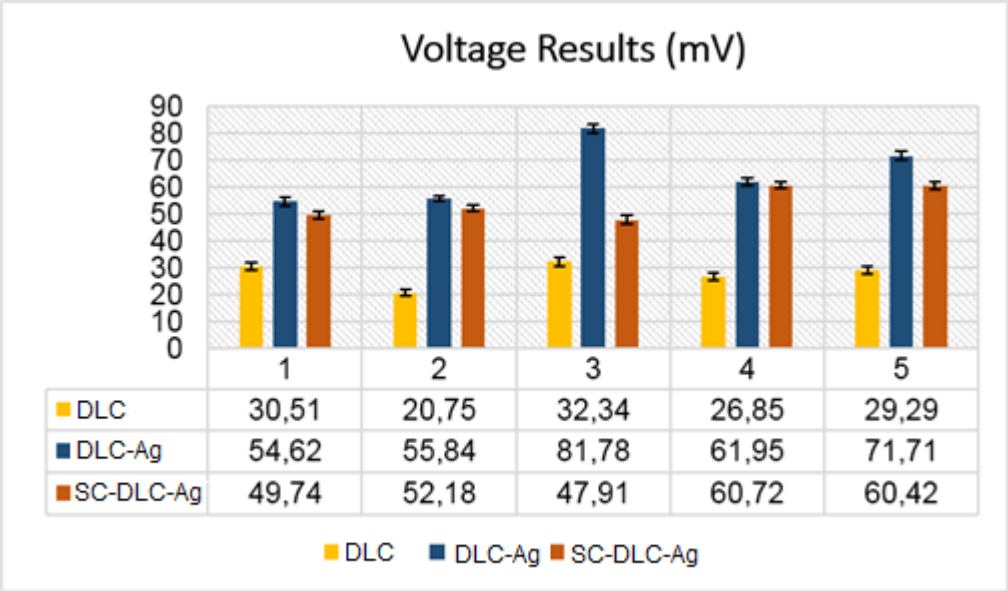

Figure 7 shows an EDX spectrum used to evaluate the presence of agglomerates of metallic silver in the film in the region of the groove (shown in Figure 6(c)). In this region, the following composition (in atomic percentages) was obtained: metallic silver (13%), carbon (89%), and silicon (5%). The silicon was derived from the Si substrate. The scattering of silver in the groove is shown by the yellow/gold shading in the AFM image. This was associated with greater variability in the electric potential of the surface, which fluctuated in the range 0.050-0.071 V (considering the maximum and minimum potentials measured along the profile). It could also be seen that the electric potential difference was higher in the region of the groove (0.049-0.068 V), compared to pure DLC. This could be mainly attributed to the ploughing effect and scattering of silver in the groove. A tribocharging effect was also observed in the regions indicated by the blue circles, which could have been due to charge dispersion and the breaking of chemical bonds caused by the movement of the tip over the film, with consequent transfer of electrons between the materials [20,21].
Electrification due to friction can occur with or without the breaking of bonds, with voltage differences caused by contact or thermoelectric effects [22,23]. On the other hand, from the perspective of mechanoemission, wear is considered as a simple plastic deformation with the breaking of adhesive and chemical bonds [24].

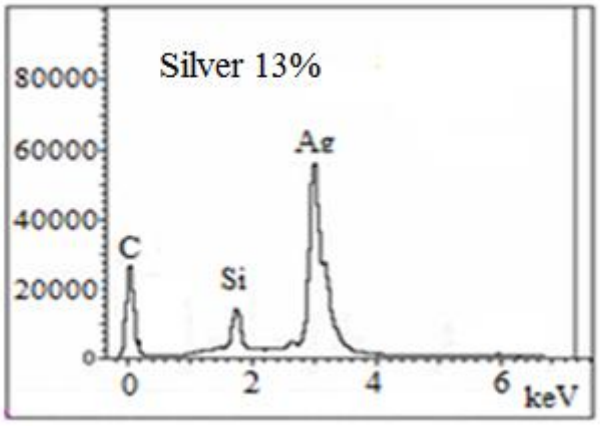

** Technical contribution to the 2nd International Brazilian Conference on Tribology – TriboBR 2014, November 3rd to 5th, 2014, Foz do Iguaçu, PR, Brazil.*

ISSN 2179-3956

Figure 7. EDX spectrum obtained for the analysis of chemical elements present in the groove region.

Figures 8(a) and 8(b) show images of the DLC-Ag film obtained using TEM and SEM, respectively. These show how the metallic silver particles were distributed in the DLC film during the deposition process. In Figure 8(a), dark particles of silver sized between 3 and 80 nm can be seen randomly distributed in the carbon film. Figure 8(c) shows an EDX spectrum spectrum obtained for an agglomerate of grains of metallic silver, revealing the presence of carbon (red stars), silicon derived from the substrate (green pentagons), and metallic silver (blue squares). The size of the silver cluster was around 40 nm. Certainly metallic silver can affect the mechanical and tribological properties of the film.

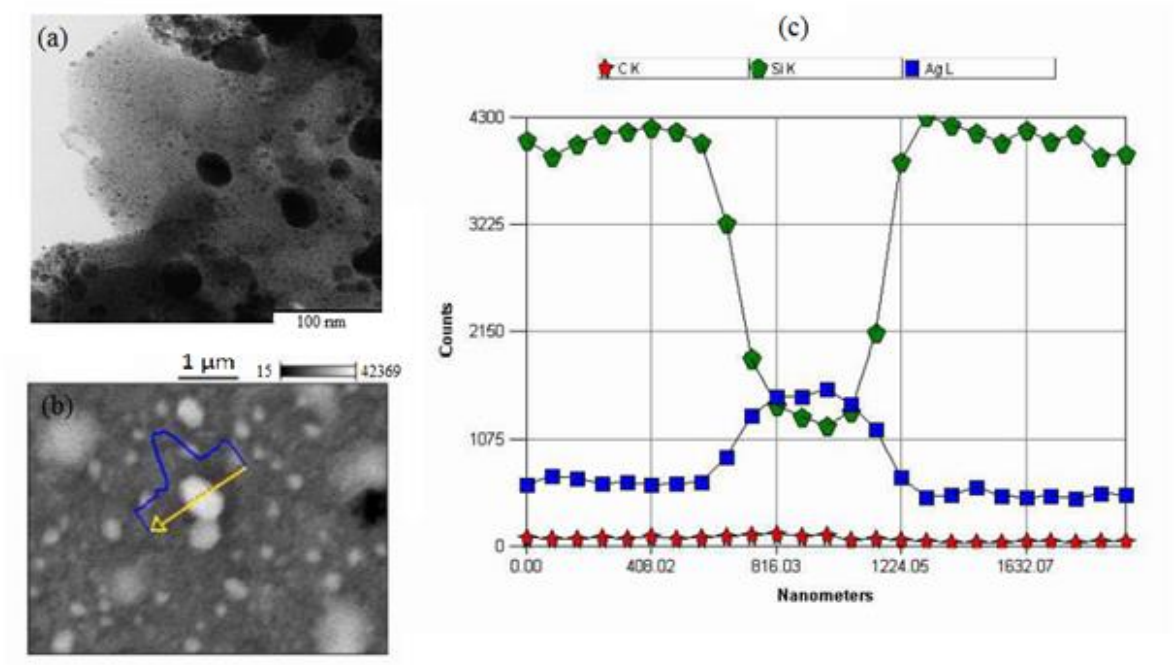

Figure 8. Images of the DLC-Ag film obtained using (a) TEM and (b) SEM, and (c) EDX spectrum of a silver agglomerate in the DLC-Ag film.

4 CONCLUSIONS

In this work, the KPFM technique was used to compare the electrostatic potential distributions on the surfaces of three different amorphous carbon films, namely DLC, DLC-Ag, and DLC-Ag with nano-scratching produced by a diamond tip. The potential mappings revealed a remarkable capacity of the silver nanoparticles incorporated in the DLC-Ag film to enhance local electrostatic charging (at the sites where they were located on the surfaces of the amorphous coatings).

Nano-scale scratching of the DLC-Ag film resulted in ploughing wear, as well as tribocharging, evidenced by the substantial enhancement of the electric field in these regions. Morphological analysis of the surface using AFM revealed the presence of silver particles spread over the DLC-Ag coating. Raman spectroscopy analysis of the coatings showed a chemical composition that was consistent with the presence of clustered carbon rings.

The random distribution of metallic silver particles in the carbon matrix reduced the friction coefficient between the diamond tip and the DLC-Ag film surface. The presence of Ag in the carbon matrix promoted the ploughing effect observed at the end of the groove, as shown in Figure 5. Effects related to tribocharging on the DLC-

* *Technical contribution to the 2nd International Brazilian Conference on Tribology – TriboBR 2014, November 3rd to 5th, 2014, Foz do Iguaçu, PR, Brazil.*

ISSN 2179-3956

Ag surface were also observed, which could be attributed to charge transfer between separate silver clusters.

Acknowledgments

The authors are grateful to C.A.R. Costa and E.M. Lanzoni (Brazilian National Nanotechnology Laboratory - LNNano). Financial support was provided by FAPESP (Pronex project number 2011/50773-0).

REFERENCES

1 Diaz A.F., Felix-Navarro R.M, A semi-quantitative tribo-electric series for polymeric materials: The influence of chemical structure and properties, J. Electrostatics 62 (2004) 277-290.
2 Singer I.L., Friction and energy dissipation at the atomic scale: A review, J. Vac. Sci. Technol. A12 (1994) 2605-2616.
3 Baytekin H.T., Patashinski A.Z., Branicki M., Baytekin B., Soh S., Grzybowski B.A., The mosaic of surface charge in contact electrification, Science 333 (2011) 308-312.
4 Burgo T.A.L., Silva C.A., Balestrin L.B.S., Galembeck F., Friction coefficient dependence on electrostatic tribocharging, Sci. Rep. UK 3 (2013) 1-8.
5 Burgo T.A.L., Ducati T.R.D., Francisco K.R., Clinckspoor K.J., Galembeck F., Galembeck S.E., Triboelectricity: macroscopic charge patterns formed by self-arraying ions on polymer surfaces, Langmuir 28 (2012) 7407-7416.
6 Nonnenmacher M., O'Boyle M.P., Wickramasinghe H.K., Kelvin probe force microscopy, Appl. Phys. Lett. 58 (1991) 2920-2923.
7 Rezende C.A., Gouveia R.F., Silva M.A., Galembeck F., Detection of charge distributions in insulator surfaces, J. Phys. Condens. Matter 21 (2009) 263002.
8 Huang J.Y., Ponce F.A., Caldas P.G., Prioli R., Almeida C.M., The effect of nanoscratching direction on the plastic deformation and surface morphology of InP crystals, J. Appl. Phys. 114 (2013) 2035031-2035039.
9 Fajardo O.Y., Mazo J.J., Surface defects and temperature on atomic friction, J. Phys. Condens. Matt. 23 (2011) 355008.
10 Radi P.A., Santos L.V., Bonetti L.F., Rodrigues G.C., Trava-Airoldi V.J., Friction and wear maps of titanium alloy against a-C:H20% (DLC) film, Surf. Coat. Tech. 203 (2008) 741-744.
11 Santos L.V., Trava-Airoldi V.J., Corat E.J., Iha K., Massi M., Prioli R., Landers R., Friction coefficient measurements by LFM on DLC films as function of sputtering deposition parameters, Diam. Relat. Mater. 11 (2002) 1135-1138.
12 Kawasegi N., Morita N., Three-dimensional lithography using combination of nanoscale processing and wet chemical etching. In: S. Hosaka (Ed.), Nanotechnology and Nanomaterials, Updates in Advanced Lithography, InTech (2013) 95-121.
13 Vieira L., Lucas F.L.C. , Fisssmer S.F., dos Santos L.C.D., Massi M., Leite P.M.S.C.M., Costa C.A.R., Lanzoni E.M., Pessoa R.S., Maciel H.S. Scratch testing for micro- and nanoscale evaluation of tribocharging in DLC films containing silver nanoparticles using AFM and KPFM techniques, in press, Surf. Coat. Tech. (2014)
14 Ogletree D.F., Carpick R.W., Salmeron M., Calibration of frictional forces in atomic force microscopy, Rev. Sci. Instrum. 67 (1996) 3298-3306.

* *Technical contribution to the 2nd International Brazilian Conference on Tribology – TriboBR 2014, November 3rd to 5th, 2014, Foz do Iguaçu, PR, Brazil.*

ISSN 2179-3956

15 Cannara R.J., Eglin M., Carpick R.W., Lateral force calibration in atomic force microscopy: A new lateral force calibration method and general guidelines for optimization, Rev. Sci. Instr. 77 (2006) 053701.
16 Sader J.E., Larson I., Mulvaney P., White L.R., Method for the calibration of atomic force microscope cantilevers, Rev. Sci. Instr. 66 (1995) 3789-3798.
17 Myshkin N.K., Petrokovets M.I., Kovalev A.V., Tribology of polymers: Adhesion, friction, wear, and mass-transfer, Tribol. Int. 38 (2005) 910-921.
18 Kriese M.D., Boismier D.A., Moody N.R., Gerbericha W.W., Nanomechanical fracture-testing of thin films, Eng. Fract. Mech. 61 (1998) 1-20.
19 Robertson J., Diamond-like amorphous carbon, Mat. Sci. Eng. 37 (2002) 129-281.
20 Gnecco E., Bennewitz R., Gyalog T., Loppacher Ch., Bammerlin M., Meyer E., Güntherodt H.-J., Velocity dependence of atomic friction, Phys. Rev. Lett. 84 (2000) 1172-1175.
21 Carpick, R.W., Salmeron, M., Scratching the surface: fundamental investigations of tribology with atomic force microscopy, Chem. Rev. 97 (1997) 1163-1194.
22 Israelachvili J.N., Tabor D., The shear properties of molecular films, Wear 24 (1973) 386-390.
23 Greason W.D., Oltean I.M., Kucerovsky Z., Ieta A.C., Triboelectric charging between polytetrafluoroethylene and metals, IEEE T. Ind. Appl. 40 (2004) 442-450.
24 Kajdas K.C., Importance of the triboemission process for tribochemical reaction, Tribol. Int. 38 (2005) 337-353.

* *Technical contribution to the 2nd International Brazilian Conference on Tribology – TriboBR 2014, November 3rd to 5th, 2014, Foz do Iguaçu, PR, Brazil.*